

# Latitudinal variations of charged dust in co-orbital resonance with Jupiter

Stefanie Reiter<sup>1</sup>  and Christoph Lhotka<sup>1,2</sup> 

<sup>1</sup>Department of Astrophysics, University of Vienna,  
Türkenschanzstrasse 17, 1180 Vienna, Austria  
email: [stefanie.reiter@univie.ac.at](mailto:stefanie.reiter@univie.ac.at)

<sup>2</sup>Department of Mathematics, University of Rome Tor Vergata,  
Via della Ricerca Scientifica 1, 00133 Rome, Italy  
email: [lhotka@mat.uniroma2.it](mailto:lhotka@mat.uniroma2.it)

**Abstract.** The interplanetary magnetic field may cause large amplitude changes in the orbital inclinations of charged dust particles. In order to study this effect in the case of dust grains moving in 1:1 mean motion resonance with planet Jupiter, a simplified semi-analytical model is developed to reduce the full dynamics of the system to the terms containing the information of the secular evolution dominated by the Lorentz force. It was found that while the planet causes variations in all orbital elements, the influence of the magnetic field most heavily impacts the long-term evolution of the inclination and the longitude of the ascending node. The simplified secular-resonant model recreates the oscillations in these parameters very well in comparison to the full solution, despite neglecting the influence of the magnetic field on the other orbital parameters.

**Keywords.** Dust dynamics, Lagrange problem, interplanetary magnetic field

---

## 1. Introduction & Background

Interplanetary space is not empty but rather filled with dust particles of various sizes. Dust grains are produced in several physical processes, i.e. the activity of the comets and collisions of asteroids, see e.g. [Koschny \*et al.\* \(2019\)](#). Additionally, dust may also be released into space via plumes (e.g. Enceladus) or by the interaction of celestial bodies with the solar wind (by sputtering and erosion). The actual origin and resulting distribution of interplanetary dust still remain an unsolved problem today. One reason for this is found in the lack of in-situ observations in large areas of interplanetary space. While observations of the zodiacal light indicate the presence of dust bands near the ecliptic plane, the presence of dust at high ecliptic latitudes can generally not be ruled out. In [Jorgensen \*et al.\* \(2020\)](#), the authors propose that a secondary population of dust at higher inclination wrt. the ecliptic is caused by scattering of a primary population at low latitudes by orbital resonances with planet Jupiter via the Kozai-Lidov (KL) effect. Alternatively, these features may be explained by dust bands that originate from a few asteroid families which deliver the dust to the inner solar system at high enough orbital inclinations – [Dermott \*et al.\* \(1984\)](#). In the present paper, we provide an alternative explanation for high latitudinal motions of small dust grains, namely via oscillations induced by the heliospheric magnetic field. Dust in space gets positively charged due to the photo-electric effect, see [Lhotka \*et al.\* \(2020\)](#). The orbital motion of charged dust results in a Lorentz force term in the equations of motion which acts normal to the orbital plane of the dust grains, leading to perturbations of the orbit. The present study

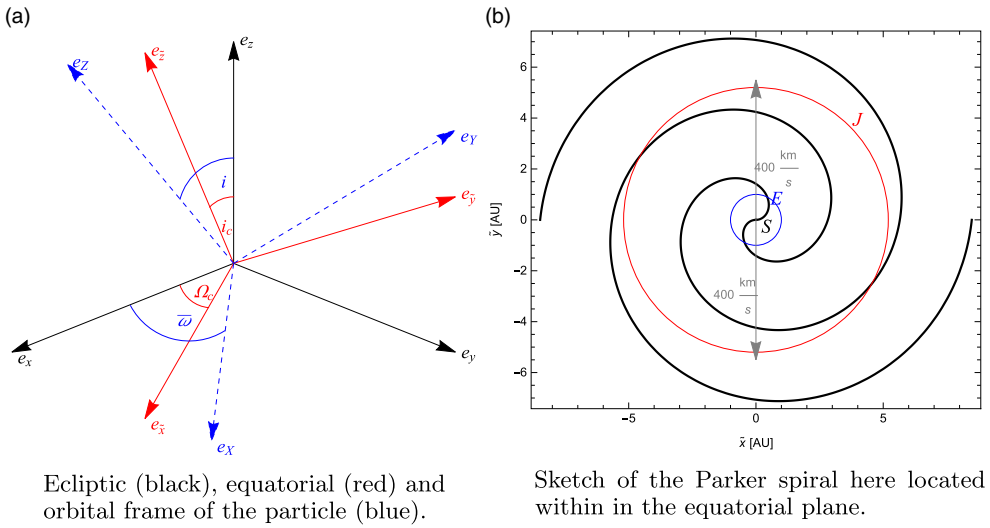


**Figure 1.** Overview of the coordinate systems and the shape of the magnetic field.

is motivated by recent findings in Liu & Schmidt (2018a), Liu & Schmidt (2018b), and can be seen as a continuation of previous studies: While the focus in Lhotka *et al.* (2016) was the role of the normal component of the interplanetary magnetic field on the radial drift of particle motions, the role of outer mean motion resonances has been investigated in Lhotka & Gales (2019). In Zhou *et al.* (2021); Lhotka & Zhou (2021) extensive numerical studies are used to investigate the role of the interplanetary magnetic field on the location and extent of the 1:1 mean motion resonance (MMR) for co-orbital dust with a planet (Jupiter and Venus), yielding interesting results on the asymmetry between the Lagrange points  $L_4$  and  $L_5$ . While these former studies heavily relied on numerical simulations, in the present work we report on the progress of deriving a semi-analytical model for co-orbital motion of dust with planet Jupiter.

Let the position vector of a micron-sized dust particle be  $\vec{r} = (x, y, z)$  in the reference frame of the ecliptic coordinate system. The rotation of the orbital frame into the ecliptic frame (a comparison between the two is given in Figure 1a) allows it to define all orbital elements, i.e. the semi-major axis  $a$ , the eccentricity  $e$ , the orbital inclination  $i$ , the argument of perihelion  $\omega$ , the longitude of the ascending node  $\Omega$ , and the mean anomaly  $M$ . Assuming that the particle is only influenced by the Sun, it would move on a Keplerian orbit with constant values for the orbital elements. The angular momentum  $h$  of the particle in this case is conserved and given by  $h = \sqrt{(1 - e^2)}a^2n$ , where  $n$  gives the mean motion of the particle. Any force (per unit mass) term beside the solar gravity is introduced into the body's equation of motion in the following way:

$$\ddot{\vec{r}} + \mu \frac{\vec{r}}{r^3} = \vec{F}, \tag{1.1}$$

with  $\ddot{\vec{r}}$  representing the acceleration vector of the particle,  $\mu$  the term  $Gm_0$  (i.e. the gravitational constant  $G$  and the solar mass  $m_0$ ), and  $\vec{F}$  an arbitrary external force (which is already assumed to be divided by particle mass in this case). Due to the influence of this perturbing force  $\vec{F}$ ,  $h$  is no longer a conserved quantity, which relates to variations in the orbital elements. It is thereby possible to derive the so-called Gauss equations – for all Kepler elements see e.g. Fitzpatrick (2016) – in the form of

$$\frac{di}{dt} = \frac{F_z r \cos(\vartheta + \omega)}{h} \qquad \frac{d\Omega}{dt} = \frac{F_z r \sin(\vartheta + \omega)}{h \sin i} \tag{1.2}$$

where  $\vartheta$  is the true anomaly. The force terms  $F_r$ ,  $F_\vartheta$  and  $F_z$  (which all appear in the full set of Gauss' equations) result from a transformation of the Cartesian force components  $F_x$ ,  $F_y$ ,  $F_z$  in the orbital system to the cylindrical coordinates in the ecliptic system, see e.g. Moulton (1914).

## 2. Dynamical model

As we are interested in studying the influence of the interplanetary magnetic field on charged particles trapped in 1:1 mean motion resonance with Jupiter, the force vector  $\vec{F}$  in (1.1) is made up of a combination of the Lorentz force and the gravitational force caused by the planet. The semi-analytical model developed from this is used to analyse the long-term effects of the Lorentz force on the orbital plane of charged dust grains (in co-orbital motion with Jupiter) in Reiter (2021). Here, we mainly focus on the development of this secular-resonant model, and its accuracy in comparison to the purely numerical approach.

For simplicity, Jupiter is placed on a circular orbit within the ecliptic plane (i.e. the  $x$ - $y$ -plane in Figure 1a). For the perturber's position vector  $\vec{r}_1$ , we therefore find  $\vec{r}_1 = (x_1, y_1, z_1) = (a_1 \cos M_1, a_1 \sin M_1, 0)$ , with  $a_1$  as the semi-major axis and  $M_1$  as the mean anomaly of the planet. For the implementation of the Lorentz force, we assume the form of the modified Parker spiral model in Webb *et al.* (2010), taking into account the dipole structure of the magnetic field. According to Parker (1958), the solar wind carries the field lines out into the solar system, and due to the solar rotation, they curl up in the shape of a spiral. This coiled-up structure of the field lines is sketched in Figure 1b. The dipole structure of the interplanetary magnetic field leads to a polarity reversal at the transition region, the so-called heliospheric current sheet. Hence, the configuration of the magnetic field depends on both the orientation of the dipole axis and the solar rotation axis, which is given by the  $\vec{e}_{\hat{z}}$ -axis of the equatorial system in Figure 1a. For simplicity, we assume that these two axes align, placing the current sheet within the equatorial plane. The equatorial coordinate system results from a rotation of the ecliptic system around the angles  $i_c$  and  $\Omega_c$ , as indicated in Figure 1a. In this work, they are fixed to  $\Omega_c = 73.5\text{deg}$  and  $i_c = 7.15\text{deg}$ , as in Beck & Giles (2005). This results in  $\vec{e}_{\hat{z}} = (x_0, y_0, z_0)$  for the expression in ecliptic coordinates. Finally, we note that we neglect the time-dependency of the magnetic field (i.e. the solar cycle).

First, we look at the implementation of the planetary perturbations into (1.1). The gravitational influence of the perturbing body on the dust grain can be defined by the potential energy  $U$  – compare e.g. Lhotka & Celletti (2015) – according to

$$U = -Gmm_1 \left( \frac{1}{\|\vec{r} - \vec{r}_1\|} - \frac{\vec{r}\vec{r}_1}{r_1^3} - \frac{1}{r} \right), \quad (2.1)$$

where  $m_1$  represents the mass of the planet. We notice that in order to obtain  $n = n_1$  at  $a = a_1$  the gravitational mass parameter  $G(m_0 + m_1)$  results in the additional term  $-1/r$  in  $U$  stemming from the potential part of the Kepler problem  $G(m_0 + m_1)/r$ , that we collect with respect to  $m_1$  in  $U$ . As for any conservative force, the perturbing force term  $\vec{F}_1$  can be derived from the gradient of the potential, i.e. via  $\vec{F}_1 = -\nabla U/m$ , for which we find:

$$\vec{F}_1 = -Gm_1 \left( -\frac{\vec{r}}{r^3} + \frac{\vec{r}_1}{r_1^3} + \frac{\vec{r} - \vec{r}_1}{\|\vec{r} - \vec{r}_1\|^3} \right), \quad (2.2)$$

Plugging (2.2) into (1.1) results in the full dynamical (Newton) solution of the influence of Jupiter. The process is similar for the implementation of the Lorentz force. Generally, the effect of the interplanetary magnetic field is expressed, see e.g. Gruen *et al.* (1994), as  $\vec{F}_L = \frac{q}{m}(\vec{v} - \vec{u}_{SW}) \times \vec{B}$ , where  $q$  is the charge of the particle,  $m$  its mass,  $\vec{v}$  its velocity,  $\vec{u}_{SW} = u_{SW}\vec{e}_r$  the velocity of the solar wind moving radially away from the

Sun $\dagger$ , and  $\vec{B}$  the magnetic field vector. The full expression of the Lorentz force used in the computations is adopted from Eq. 16 in Lhotka & Gales (2019) in the form of

$$\vec{F}_L = -\frac{qB_0r_0^2}{mr^2} \left( \frac{\vec{r} \times \dot{\vec{r}}}{r} + \frac{\Omega_s}{r} \vec{r} \times (\vec{r} \times \vec{e}_z) + \frac{\Omega_s}{u_{SW}} (\vec{r} \times \vec{e}_z) \times \dot{\vec{r}} \right) \tanh \left( \frac{\alpha r \vec{e}_z}{r} \right), \quad (2.3)$$

where  $B_0$  gives the background magnetic field strength at a reference distance of  $r_0$  (typically 1AU), and  $\Omega_s$  represents the solar rotation rate. The unit vector  $\vec{e}_z$  yields the  $\tilde{z}$ -direction in the equatorial system, so it represents both the dipole and the rotation axis of the Sun, as already explained above. Finally, the parameter  $\alpha$  is used to model the sign change of the magnetic field at the solar equator (i.e. it represents the effect at the heliospheric current sheet). Combining (2.3) and (2.2) into (1.1) as  $\vec{F} = \vec{F}_1 + \vec{F}_L$  describes the numerical approach for the particle dynamics.

As we are primarily interested in studying the secular evolution of the particle analytically rather than numerically, it is necessary to express the force terms (2.2) and (2.3) in cylindrical coordinates and plug the resulting values for  $F_r$ ,  $F_\vartheta$  and  $F_z$  into all Gauss equations exemplified in (1.2). Starting again with the influence of the perturbing body, it is beneficial to expand the potential  $U$ , i.e. (2.1), into small parameters ( $e$  and  $\rho = r/r_1 - 1$ ) and the angle  $\cos \psi = \frac{r\vec{r}_1}{rr_1}$  between the two position vectors. The gradient of this expression is then used to compute the cylindrical vector components. For more details on this series expansion, see Lhotka & Celletti (2015). This computation is advantageous, as it facilitates isolating the secular terms from the full solution and hence from the short-period oscillations induced by  $M$ . With the example of  $a$ , we note that the terms for the long-term evolution of each orbital element take the form of a Fourier series according to

$$\frac{da}{dt} = \sum_{k=0}^K \sum_{l=0}^L \sum_m^{M'} c_{klm}^{(a)}(e) \cos(ki) \sin(l\Phi + m\omega), \quad (2.4)$$

where  $\Phi = M + \omega + \Omega - M_1$  is the resonant angle – see e.g. Beauge (1994) – and  $c$  denotes polynomials in  $e$ . The three orders of expansion ( $k, l, m$ ) occur due to the expression of  $U$  in terms of  $e, \rho$  and  $\cos(\psi)$ . A comparison of the results from the full solution in terms of the planetary perturbations using the Newton equations – i.e. (2.2) in (1.1) – and of the secular evolution from the Gauss equations is given in Figure 2.

As for the influence of the interplanetary magnetic field, (2.3) also needs to be implemented into all Gauss equations, from e.g. Fitzpatrick (2016). In Lhotka & Gales (2019), the authors have been able to isolate those terms of the equations, which do not average out on longer timescales, from the full solution. As it was solely the normal component of the magnetic field causing long-term oscillations, only  $i$  and  $\Omega$  are the dynamically relevant terms for our semi-analytical model. The equations of Lhotka & Gales (2019) are implemented here in the form of

$$\frac{di}{dt} = -\alpha \frac{qB_0}{2m} \left( \frac{r_0}{a} \right)^2 \left( \left( 1 - z_0 \cos i \frac{\Omega_s}{n} \right) (x_0 \cos \Omega + y_0 \sin \Omega) \right) \quad (2.5)$$

$$\begin{aligned} \frac{d\Omega}{dt} = & -\alpha \frac{qB_0}{2m} \left( \frac{r_0}{a} \right)^2 \left( \left( \cot i - z_0 \frac{\Omega_s \cos(2i)}{n \sin i} \right) (y_0 \cos \Omega - x_0 \sin \Omega) \right. \\ & \left. + \cos i (1 - 2z_0) \frac{\Omega_s}{n} + z_0 \right), \end{aligned} \quad (2.6)$$

$\dagger$  Due to the combination of a so-called frozen-in magnetic field and no background current resistivity (Lhotka *et al.* (2016)), the solar wind vector appears due to the form of the electric field vector  $\vec{E} = -\vec{u}_{SW} \times \vec{B}$ .

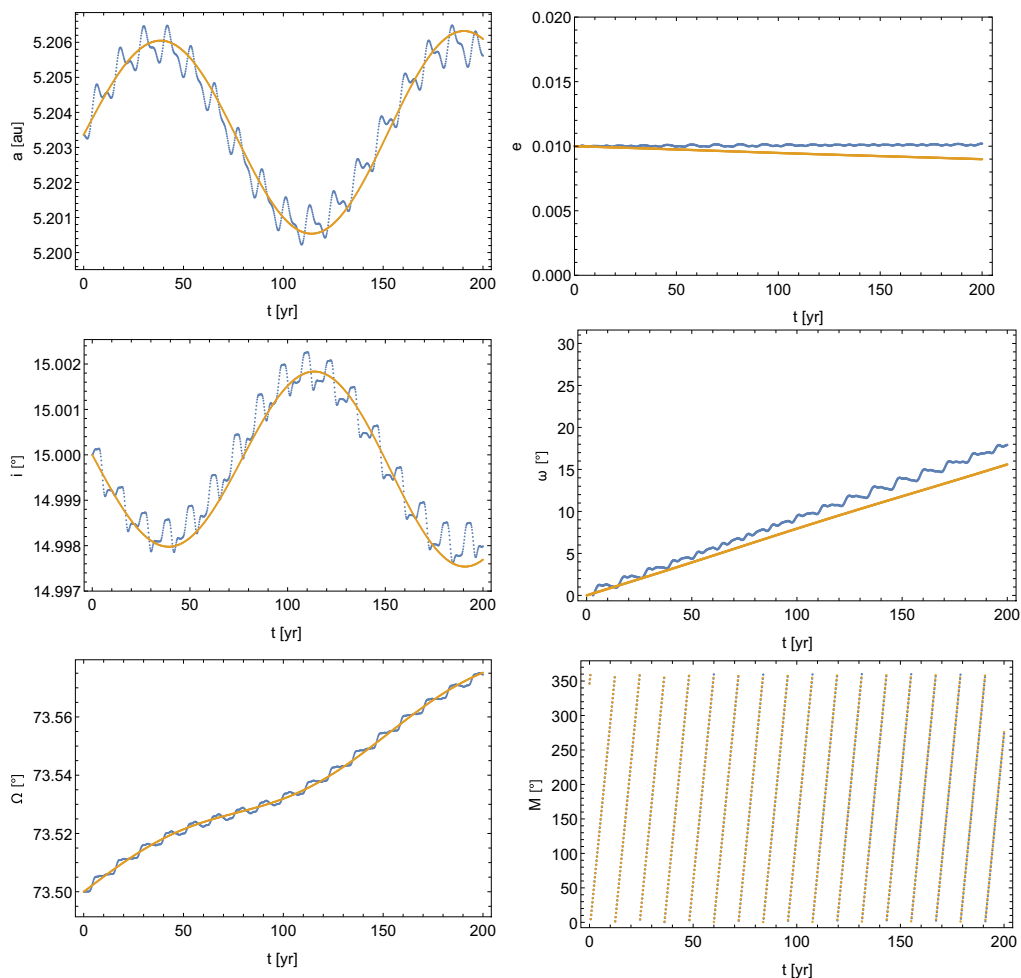


**Figure 2.** Comparison of the Newton solution (blue) and the resonant secular model (yellow) for uncharged particles in 1:1 mean motion resonance with Jupiter.

where  $\vec{e}_z = (x_0, y_0, z_0)$ . The combination of these two expressions with the resonant terms resulting from the Gauss equations in the form of (2.4) yields the secular dynamics of a charged dust particle in co-orbital motion with Jupiter, as it is affected by the magnetic field. As we only implement the effect of the Lorentz force on the inclination and the longitude of the ascending node into the model, we limit the analysis of the dynamics to the parameter space of  $i$  and  $\Omega$ . Figure 3 shows that in the case of these two orbital elements, the agreement between the full Newton solution and the approximated Gauss model is very good. A comparison of the results in Figure 3 and the middle and lower left graphs in Figure 2 indicates that the magnetic field, rather than the influence of Jupiter, governs the secular dynamics in the  $i$ - $\Omega$ -space. The results demonstrate that the semi-analytical model comprised of (2.5) and (2.6) in combination with (2.4) for all orbital elements is very useful for analysing the long-term evolution of the orbital plane of charged dust grains in 1:1 mean motion resonance with Jupiter, as is done in detail in Reiter (2021). Most notably, we find that the latitudinal motion of micron-sized dust can easily be explained by the Lorentz force stemming from the interaction of micron-sized charged dust with the heliospheric magnetic field. A study on the dynamics in the full

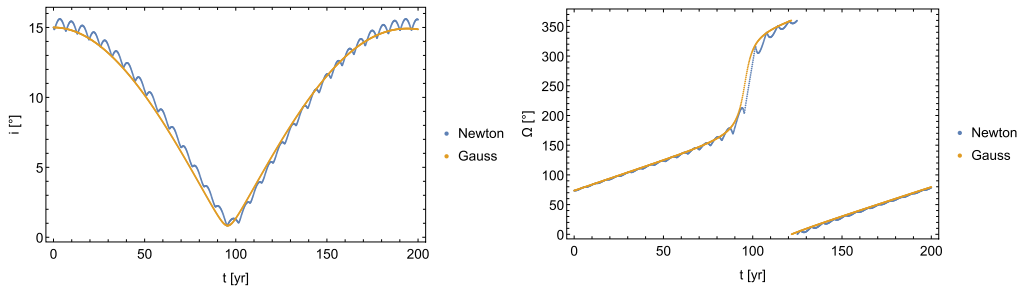


**Figure 3.** As Figure 2 for the inclination  $i$  and the longitude of the ascending node  $\Omega$ , but in the case of a charged dust grain affected by both Jupiter and the interplanetary magnetic field.

$(\Omega, i)$ -plane for charged dust of varying particle size, and located at different regions in the solar system is currently in progress.

### Acknowledgments

This work is fully supported by the Austrian Science Fund FWF with project number P-30542.

### References

- Beauge, C. 1994, *Celestial Mechanics and Dynamical Astronomy*, 60, 225
- Beck, J. G. & Giles, P. 2005, *ApJ*, 621, L153
- Dermott, S.F., Nicholson, P.D., Burns, J.A., Houck, J.R. 1984, *Nature*, 312, 505
- Fitzpatrick, R. 2016, *An Introduction to Celestial Mechanics*
- Gruen, E., Gustafson, B., Mann, I., et al. 1994, *AAP*, 286, 915
- Jorgensen, J.L., Benn, M., Connereny, J.E.P., Denver, T., Jorgensen, P.S., Andersen, A.C., and Bolton, S.J 2020, *JGR Planets*, 126, e2020JE006509
- Koschny, D., Soja, R. H., Engrand, C., et al. 2019, *Space Sci. Revs*, 215, 34
- Lhotka, C., Zhou, L. 2021, *CNSNS*, <https://doi.org/10.1016/j.cnsns.2021.106024> (accepted)
- Lhotka, C. & Celletti, A. 2015, *Icarus*, 250, 249
- Lhotka, C., Bourdin, P., Narita, Y. 2016 *ApJ*, 828, 10
- Lhotka, C. & Gales, C. 2019, *Celestial Mechanics and Dynamical Astronomy*, 131, 49
- Lhotka, C., Rubab, N., Roberts, W.W., Holmes, J., Torkar, K., Nakamura, R. 2020 *PoP*, 27, 103704
- Liu, X. & Schmidt, J. 2018, *A&A*, 609, A57
- Liu, X. & Schmidt, J. 2018, *A&A*, 614, A97
- Moulton, F. R. 1914, *An introduction to celestial mechanics* (New York, The Macmillan company)
- Parker, E. N. 1958, *ApJ*, 128, 664
- Reiter, S. 2021, *The spatial distribution of charged dust particles in the outer solar system*, (University of Vienna, in preparation)
- Webb, G. M., Hu, Q., Dasgupta, B., et al. 2010, *Journal of Geophysical Research (Space Physics)*, 115, A10112
- Zhou, L., Lhotka, C., Gales, C., Narita, Y., Zhou, L.-Y. 2021, *A&A*, 645, A63